Electronic Supplementary Material (ESI) for Nanoscale.

Electronic Supporting Information

Transition Metal/Nitrogen dual-doped Mesoporous Graphene-like Carbon Nanosheets for Oxygen Reduction and Evolution reactions

Xiaobo Liu, Ibrahim Saana Amiinu, Shaojun Liu, Kun Cheng， Shichun Mu*

State Key Laboratory of Advanced Technology for Materials Synthesis and Processing, Wuhan University of Technology, Wuhan, 430070, PR China

E-mail: msc@whut.edu.cn

List of figure captions

Scheme S1 Shape evolution from NC (a) to Co@N-PC (b), Co@N-PGCS (c). Briefly, NC displays amorphous carbon structure, after addition of cobalt salts, surface roughness increases, and Co species can convert the amorphous carbon to more regular graphitic carbon, some Co species embedded ultra-thick graphitic carbon layer are difficult removed completely (Co@N-PC). For Co@N-PGCS, the pyrolysis production (MgO) of $Mg(OH)_2$ at high temperature can serve as template, contribute to the formation of mesoporous structure with thin shell.

Figure S1 (a) FESEM image of NC; (b) HRTEM images of NC which exhibits an amorphous characteristic; (c) and (d) TEM images of Co@N-PGCS at different magnification scale and district.

Figure S2 (a) TEM images of Co@N-PGCS with highly porous structure; (b) TEM image of Co@N-PC which the Co_3O_4 encapsulated in ultra-thick graphitic carbon layer.

Figure S3 Simultaneous thermal analysis of Co@N-PGCS.

Figure S4 (a) XPS survey of NC through direct thermal decomposition of chitosan; (b) C1s; (c) N1S. (d) XPS survey of Co@N-PC; (e) C1s; (f) N1s; (g) Co2p.

Figure S5 The current vs. time (i – t) chronoamperometric responses of Co@N-PGCS and Pt/C: (a) Durability, inset: the ratio of the current loss (J/J_0), (b) Methanol tolerance (1 M), inset: the ratio of the current loss (J/J_0), and (c) CO tolerance (≈10%)， inset: the ratio of the current loss (J/J_0). (d) and (e) LSV curves of Co@N-PGCS and Pt/C separately, the stability of catalysts was symbolized by$\triangle E_{1/2}$ before and after the i – t test. Data (a, b, c, d and e) were recorded in 0.1 M KOH solution in O_2-saturated at a constant potential at -0.30 V and a rotation speed of 1600 rpm, (f) Comparison of ORR performance for Co@N-PGCS and commercial Pt/C in O_2-saturated 0.1 M $HClO_4$ solution with a rotation speed of 1600 rpm.

Figure S6 (a) Survey statistics of onset potential and half-wave potential for NC, Co@N-PC, Co@N-PGCS, and NC; (b) Electron transfer number of Co@N-PGCS.

For ORR, the average number of electrons transferred is estimated using the Koutecky-Levich equation. [1]

$$\frac{1}{j} = \frac{1}{j_k} + \frac{1}{j_L} = \frac{1}{B\omega^{1/2}} + \frac{1}{j_k}$$

$$B = 0.62nFC_0(D_0)^{2/3}\nu^{-1/6}$$

where n is the electron transfer number , j indicates measured current density, j_k is the kinetic current density, j_L is the diffusion-limited current density, ω is the speed of electrode rotation, F denotes the Faraday constant (F = 96485 C mol^{-1}), C_0 is the bulk oxygen concentration (C_0 =1.2×10^{-3} mol L^{-1}), D_0 is the diffusion coefficient of oxygen (D_0 =1.9×10^{-5} cm^2 s^{-1} in 0.1M KOH) and ν is the kinematic viscosity of the solution (ν = 1.0×10^{-2} cm^2 s^{-1}).

Figure S7 Nyquist plots of NC, Co@N-PC, and Co@N-PGCS modeled by equivalent electrical circuit (inset).

Figure S8 (a) i-t curves of Co@N-PGCS at a constant potential of 0.65V. Inset pictures are bubble size at different time. (b) i-t curves of Co@N-PGCS at a rotation speed of 1600rpm.

Table S1 Elemental contents of samples by Element Mapping and XPS surface scan.

Scheme S1

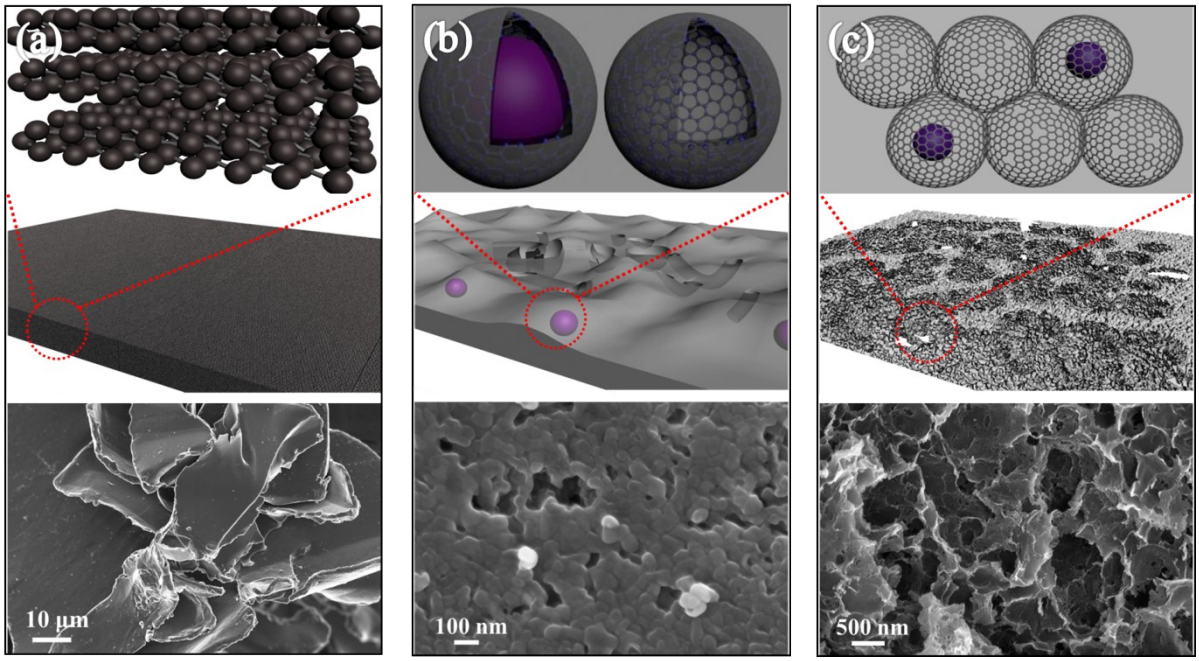
(a)
10 μm
(b)
100 nm
(c)
500 nm

Figure S1

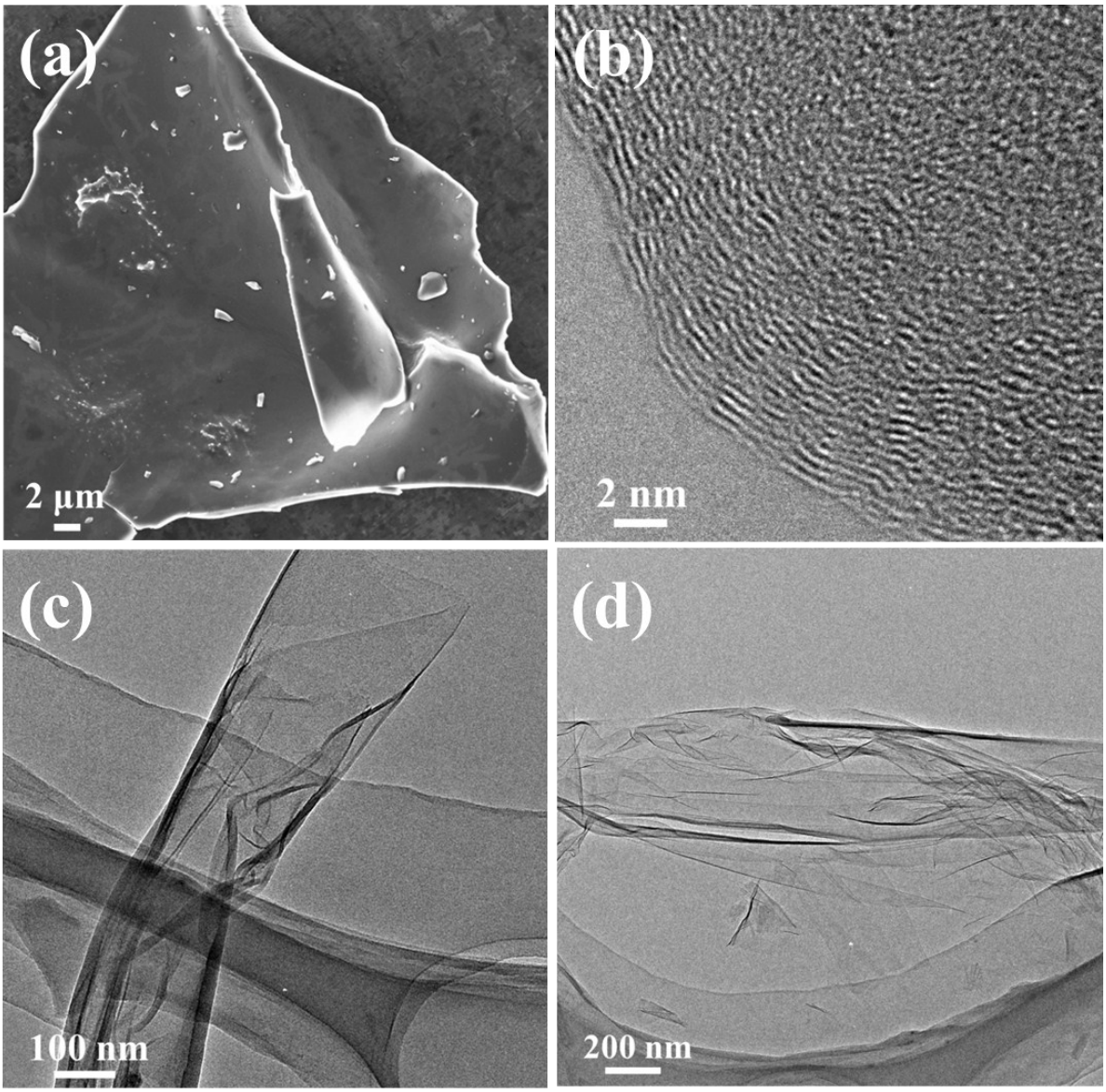

Figure S2

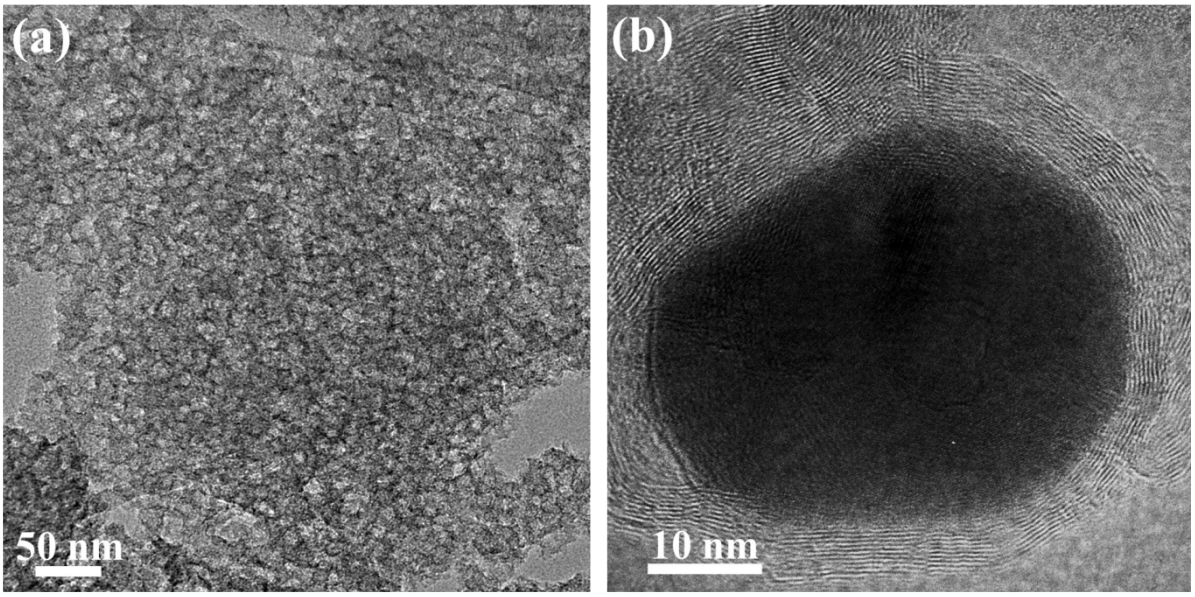

Figure S3

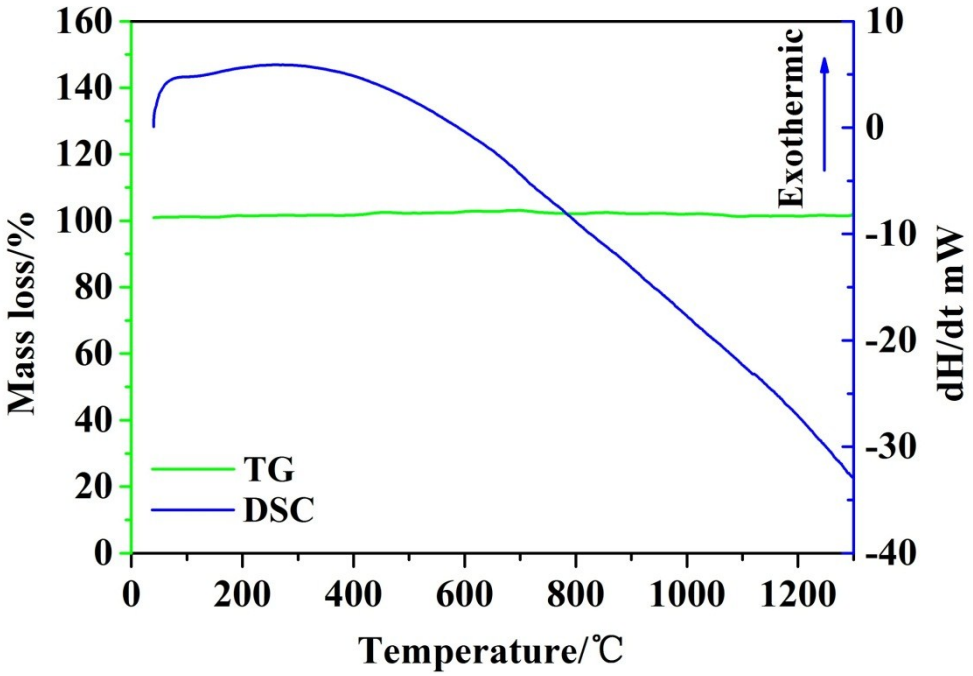
Mass loss/%
dH/dt mW
Temperature/℃
TG
DSC
Exothermic
160
140
120
100
80
60
40
20
0
10
0
-10
-20
-30
-40
0
200
400
600
800
1000
1200

Figure S4

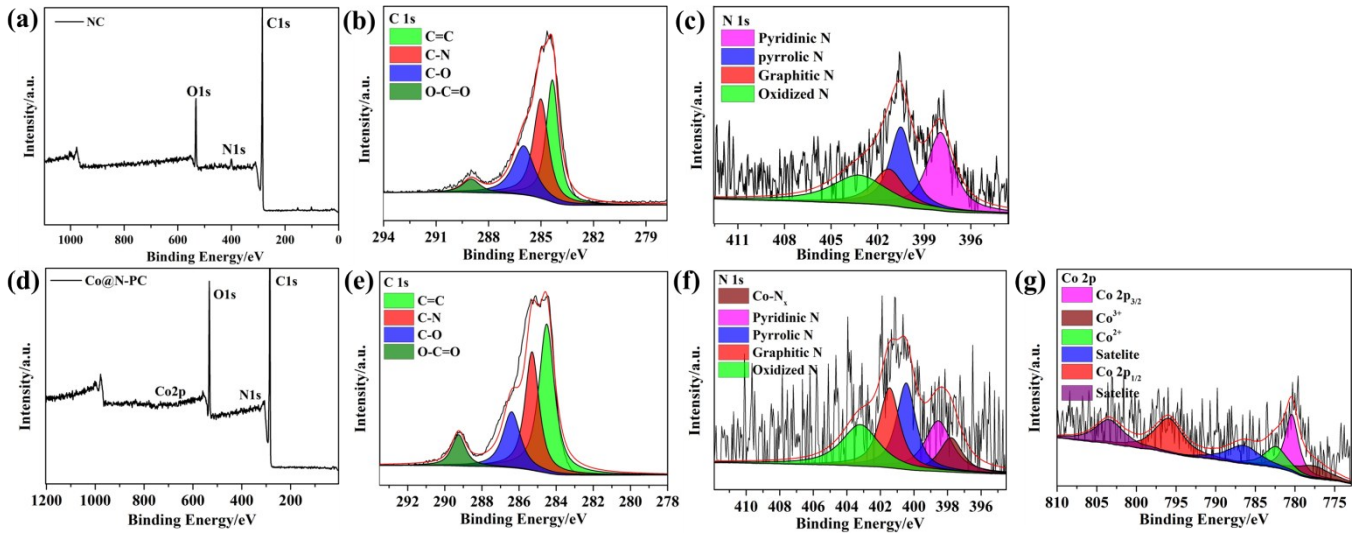
(a)
NC
C1s
O1s
N1s
Intensity/a.u.
Binding Energy/eV
(b)
C 1s
C=C
C-N
C-O
O-C=O
Intensity/a.u.
Binding Energy/eV
(c)
N 1s
Pyridinic N
pyrrolic N
Graphitic N
Oxidized N
Intensity/a.u.
Binding Energy/eV
(d)
Co@N-PC
C1s
O1s
Co2p
N1s
Intensity/a.u.
Binding Energy/eV
(e)
C 1s
C=C
C-N
C-O
O-C=O
Intensity/a.u.
Binding Energy/eV
(f)
N 1s
Co-Nx
Pyridinic N
Pyrrolic N
Graphitic N
Oxidized N
Intensity/a.u.
Binding Energy/eV
(g)
Co 2p
Co 2p3/2
Co3+
Co2+
Satelite
Co 2p1/2
Satelite
Intensity/a.u.
Binding Energy/eV

Figure S5

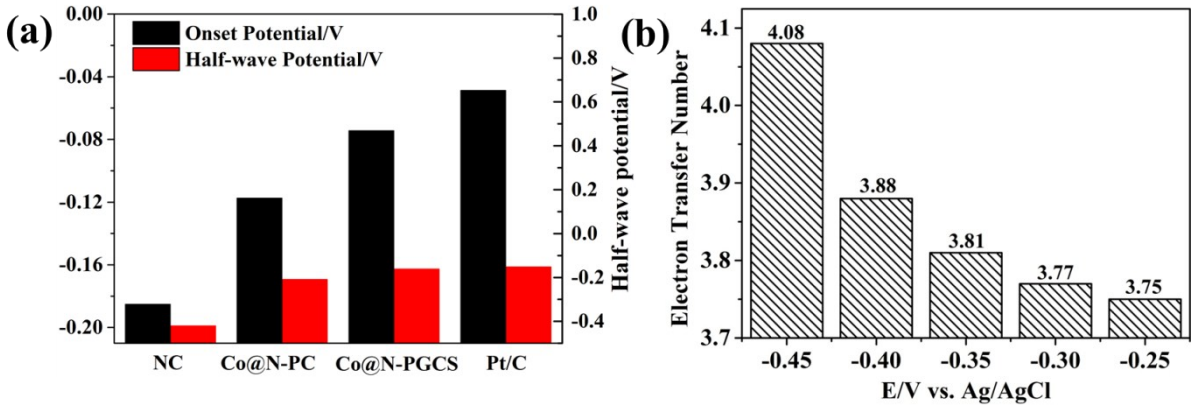
(a)
Onset Potential/V
Half-wave Potential/V
0.00
-0.04
-0.08
-0.12
-0.16
-0.20
1.0
0.8
0.6
0.4
0.2
0.0
-0.2
-0.4
Half-wave potential/V
NC
Co@N-PC
Co@N-PGCS
Pt/C
(b)
Electron Transfer Number
4.1
4.0
3.9
3.8
3.7
4.08
3.88
3.81
3.77
3.75
-0.45
-0.40
-0.35
-0.30
-0.25
E/V vs. Ag/AgCl

Figure S6

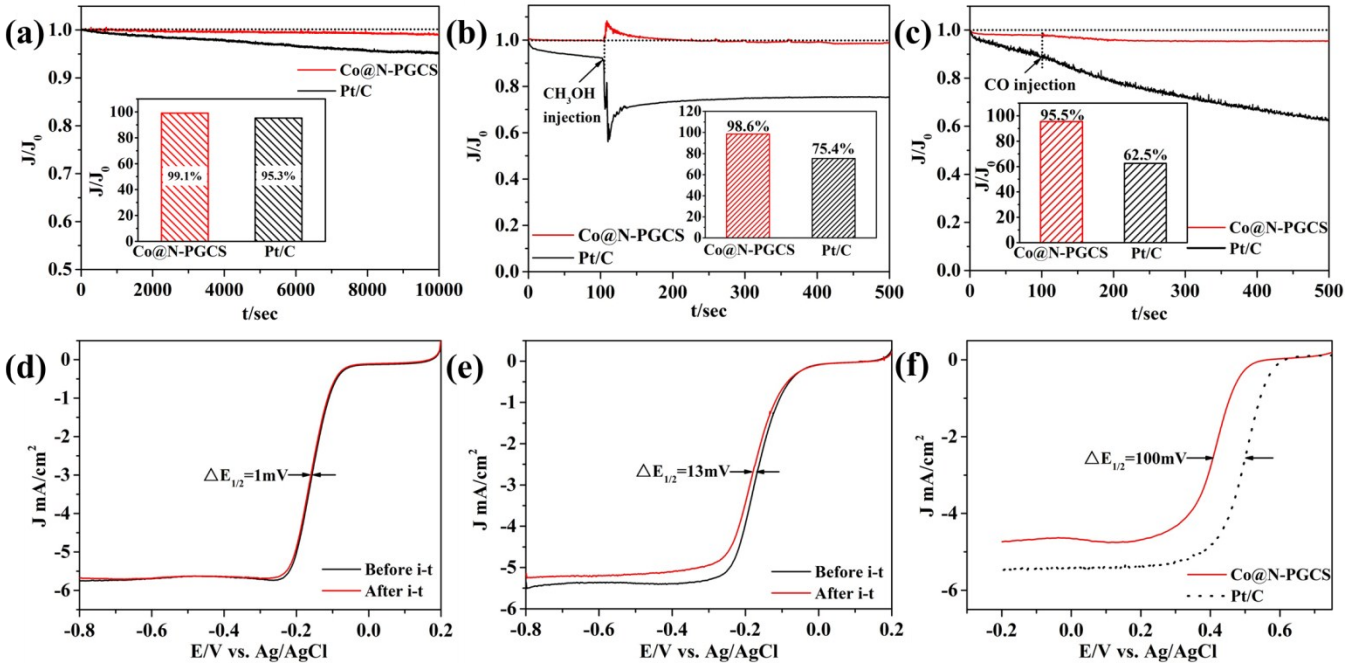
(a)
Co@N-PGCS
Pt/C
J/J0
t/sec
99.1%
95.3%
Co@N-PGCS
Pt/C
(b)
CH3OH injection
Co@N-PGCS
Pt/C
98.6%
75.4%
(c)
CO injection
95.5%
62.5%
(d)
△E1/2=1mV
Before i-t
After i-t
J mA/cm2
E/V vs. Ag/AgCl
(e)
△E1/2=13mV
(f)
△E1/2=100mV

Figure S7

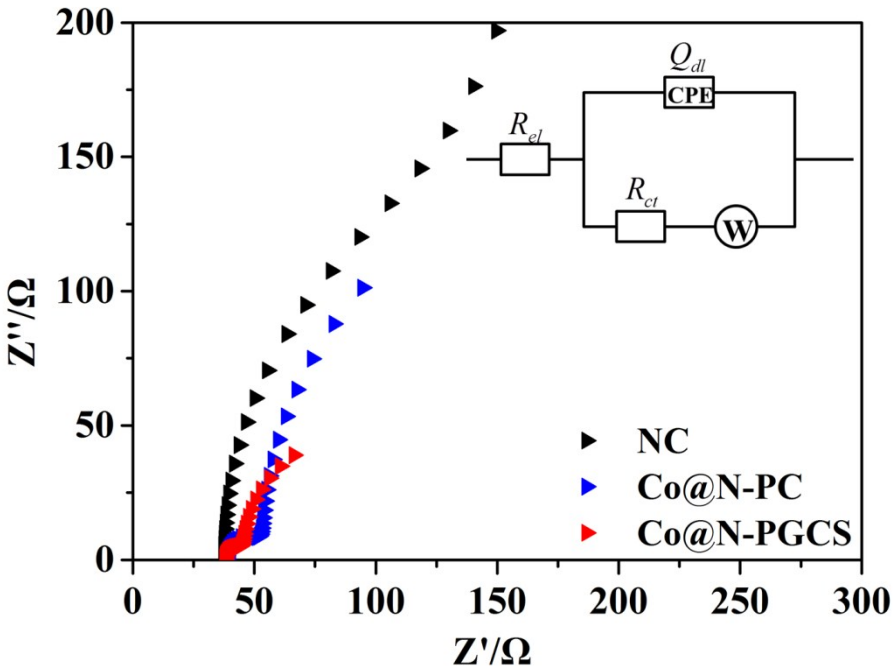
200
150
100
50
0
Z''/Ω
0
50
100
150
200
250
300
Z'/Ω
Q_{dl}
CPE
R_{el}
R_{ct}
W
NC
Co@N-PC
Co@N-PGCS

Figure S8

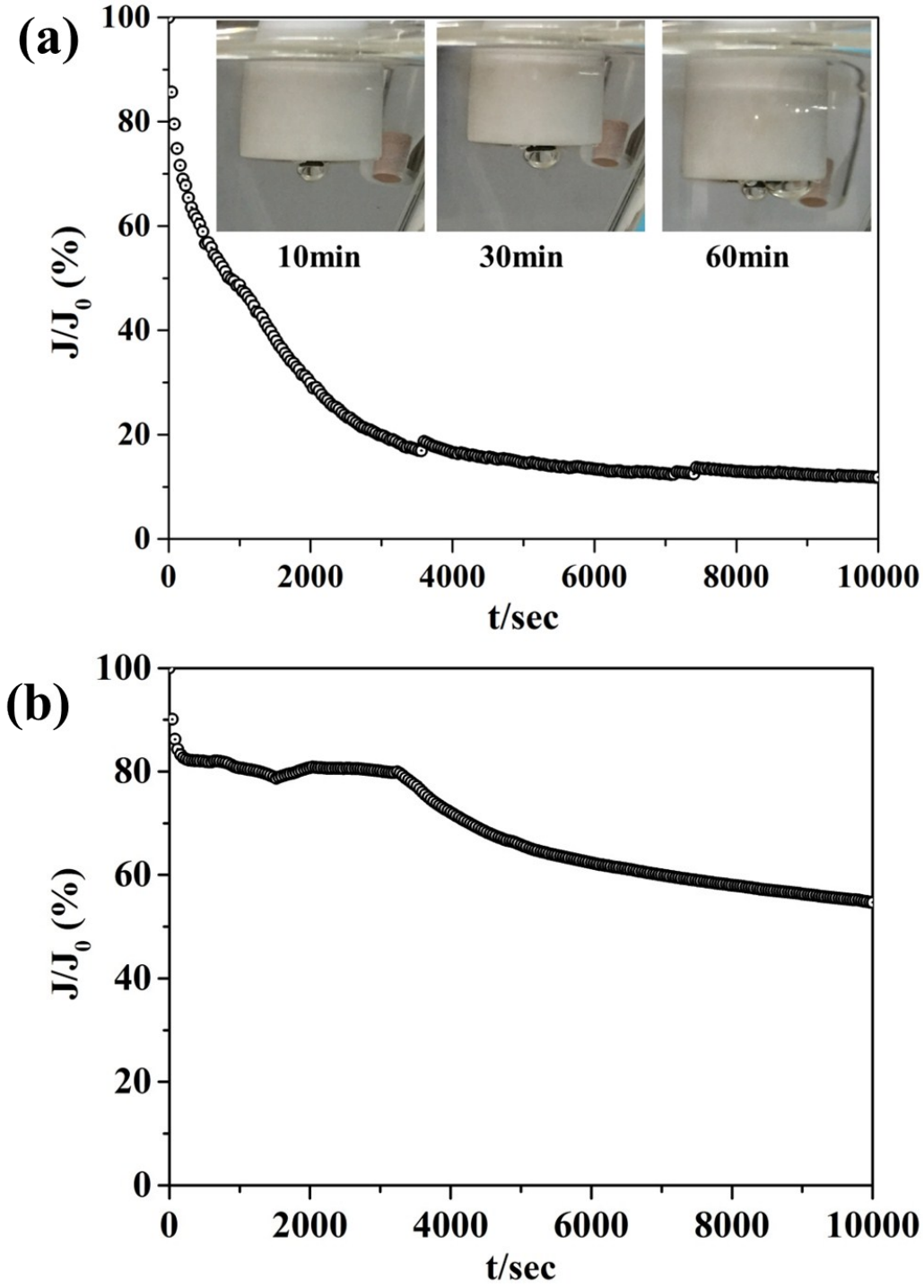

Table S1

Element	XPS (at. %)			Element Mapping (wt. %)
	NC	Co@N-MPG	Co@N-PG	Co@N-MPG
C	84.75	94.12	86.29	87.72
O	12.61	3.69	13.56	6.37
N	2.65	2.13	0.05	2.67
Co	–	0.06	0.1	3.23

Reference

1 Chen, Z., Higgins, D., Chen, Z. *Carbon*, 2010, **48**, 3057.